View metadata, citation and similar papers at core.ac.uk

brought to you by CORE

provided by NASA Technical Reports Server

NASA Technical Paper 3630

Calculation of Heavy Ion Inactivation and Mutation Rates in Radial Dose Model of Track Structure

Francis A. Cucinotta and John W. Wilson
Langley Research Center • Hampton, Virginia

Mark R. Shavers
Texas A&M University • College Station, Texas

Robert Katz
University of Nebraska • Lincoln, Nebraska

National Aeronautics and Space Administration
Langley Research Center • Hampton, Virginia 23681-2199

July 1997

Available electronically at the following URL address: http://techreports.larc.nasa.gov/ltrs/ltrs.html

Printed copies available from the following:

NASA Center for AeroSpace Information
800 Elkridge Landing Road
Linthicum Heights, MD 21090-2934
(301) 621-0390

National Technical Information Service (NTIS)
5285 Port Royal Road
Springfield, VA 22161-2171
(703) 487-4650

Summary

In the track structure model, the inactivation cross section is found by summing an inactivation probability over all impact parameters from the ion to the sensitive sites within the cell nucleus. The inactivation probability is evaluated by using the dose response of the system to gamma rays and the radial dose of the ions and may be equal to unity at small impact parameters. We apply the track structure model to recent data with heavy ion beams irradiating biological samples of *E. Coli*, *Bacillus Subtilis* spores, and Chinese hamster (V79) cells. Heavy ions have observed cross sections for inactivation that approach and sometimes exceed the geometric size of the cell nucleus in mammalian cells. We show how the effects of inactivation may be taken into account in the evaluation of the mutation cross sections from heavy ions in the track structure model through correlation of sites for gene mutation and cell inactivation. The model is fit to available data for HPRT (hypoxanthine guanine phosphoribosyl transferase) mutations in Chinese hamster cells, and good agreement is found. The resulting calculations qualitatively show that mutation cross sections for heavy ions display minima at velocities where inactivation cross sections display maxima. Also, calculations show the high probability for mutation by relativistic ions due to the radial extension of the ion track from delta rays in agreement with the microlesion concept. The effects of inactivation on mutation rates make it very unlikely that a single parameter such as LET (linear energy transfer) or Z^{*2}/β^2 (where Z^* is effective charge number and β is ion velocity) can be used to specify radiation quality for heavy ion bombardment.

Introduction

The level of biological injury expected from galactic cosmic rays (GCR) during prolonged manned spaceflight is difficult to estimate because of the lack of human data from exposures to high charge and energy (HZE) particles. Experimental studies for estimating the risk from long-term GCR exposures include track segment irradiations with HZE particles in which animals or cell cultures are used. The most useful end points for such studies with animals are cancer induction and mortality. Cellular studies using cytotoxicity as an end point are useful for providing estimates of the relative biological effectiveness (RBE); the stochastic end points of mutagenesis or neoplastic transformation provide additional information on the late effects that may be useful in extrapolations of the level of risk for man and on the underlying mechanisms of damage from HZE particles. Studies for stochastic end points, in vitro, are ultimately limited by the multistep nature of carcinogenesis (Weinberg 1991; Vogelstein and Kinzler 1993). Although it is unclear if carcinogens, including radiation, cause one or several mutagenic changes in the pathways of tumor formation or if a mutator phenotype is induced (Loeb 1991; Little 1994) leading to genomic instability, the implications are that RBEs derived from one-step processes may be limited. In fact, the hypothesis exists that RBEs for tumor formation in protracted exposures may approach the RBE for a one-step process raised to the power of the number of mutations observed in cancer formation and is suggested by some studies (Ullrich 1984) where large RBEs are found. For defining radiation quality of heavy ion beams the parameter linear energy transfer (LET) is expected to be insufficient due to track structure effects. We consider through comparisons with experiments the use of the track structure model for determining the radiation quality of ion beams for in vitro studies.

The track structure model was first used to describe heavy ion inactivation cross sections by Butts and Katz (1967) and has continued success in describing radiobiological data with heavy ion beams since that time. In the track model, the spatial distribution of energy about an ion is used to map the response of low LET irradiations, such as gamma rays or electrons, to that of an ion. An inactivation probability as a function of impact parameter or radial distance about the ion can be described in this manner by using the ion radial dose and the gamma-ray response function. For a finite target size, the radial dose is averaged over the target volume assumed to be a short cylinder of radius a_{0I}. Several experiments have now been performed (Facius et al. 1983; Weisbrod et al. 1992) to measure the inactivation probability $P(t)$ for ion bombardment of *Bacillus subtilis* spores. These measurements appear to indicate that the probability is not unity for small impact parameters for uranium bombardments; this indication seems to contradict the predictions of the track structure model. Recently, calculations for the inactivation probability of spores (Cucinotta et al. 1995) have shown that, if the sensitive targets in the spores are allowed to be displaced from the center of the spore volume, a good representation of these measurements is provided by the track model, and a unit probability for small impact parameters is not ruled out. Recent measurements of the DNA (deoxyribonucleic acid) content in yeast cells by Kost and Kiefer (1993) also support the assertion that the impact parameters in the inactivation measurements are likely to be displaced from the sensitive site for inactivation.

An experimental assay has been developed for studies of mutations at the hypoxanthine guanine phosphoribosyl transferase (HPRT) locus in mammalian cell cultures. The HPRT gene is located on the X chromosome, and the mutation of this gene is related to DNA damage. The HPRT mutation assay is used to study large

deletions or rearrangements by ionizing radiation (National Council on Radiation Protection Measurements (NCRP) 1990). This assay system has been used by several groups with a variety of light and heavy ion types in several cell lines (Thacker, Stretch, and Stephens 1979; Cox and Masson 1979; Kronenberg and Little 1989; Kranert, Schneider, and Kiefer 1990). One of the shortcomings of this assay system is that the chromosome involved is necessary for cell replication, which results in the loss of potential mutants. Human-hamster hybrid systems are being used to obtain higher mutation rates in other studies (NCRP 1990). Also, measurements (Kronenberg and Little 1989) of mutations to trifluorothymidine resistance locus indicate slow-growth mutants that are not typical of the HPRT mutants, an indication that some variability exists in mutations at specific genetic loci in human cells.

In describing mutagenesis from heavy ions, the question arises of whether there will be any mutations observed at all if single tracks of heavy ions kill the cell due to the large energy they deposit in the cell nucleus. Goodhead et al. (1980) and Kranert, Schneider, and Kiefer (1990) have discussed this problem noting that for heavy ions, the inactivation cross section is generally smaller than the nuclear area for mammalian cells and that track structure effects should be considered in order to understand the role of inactivation on heavy ion mutagenesis. Studies by Lett, Cox, and Story (1989) with repair deficient LS1784 S/S cells show that inactivation cross sections may exceed the geometric cross section sometimes. We use the track structure model of Katz et al. (1971) and Katz, Dunn, and Sinclair (1985) in order to evaluate the mutation cross section for ion bombardment of Chinese hamster fibroblasts (V79). We show that the mutation cross sections for ions throughout the periodic table can be described by the track model when inactivation effects are accounted for in the model. In effect, we will have a qualitative model of what has long been suggested (Grahn 1973; Todd 1983; Kiefer 1993) of heavy ion mutagenesis, including the concept of a microlesion where mutated cells surround a core of inactivated ones.

The experimental data for the dose response for mutations from gamma rays in mammalian cells are severely limited. Data below doses of 0.5 Gy are difficult to obtain because of poor statistics. Data above doses of 10 Gy are also difficult to obtain because of the high inactivation rates leading to poor recovery of mutants. The track structure model relies on extrapolating effects of low LET irradiations at high dose rate to that of ions using the low LET dose response. The extrapolation becomes difficult because of the limited range of data for the dose response. The track model employs a multitarget or multihit model for the functional form of the dose response. Wilson, Cucinotta, and Shinn (1993) have developed a linear repair/misrepair kinetics model for multiple lesion formation appropriate for mutation in competition with inactivation. We consider both the multitarget and linear kinetics model for the low LET dose response model.

Our accounting of inactivation effects on heavy ion mutation cross sections relies on the assumption that the sensitive sites for inactivation may be displaced from that of mutation. We average the displacement distance over the nuclear volume for the V79 cells; this leads to a good representation of the existing measurements of mutation cross sections in V79 cells. Parameters for cell inactivation are fixed in the model from inactivation data. The resulting model shows, in agreement with the data, that the mutation cross section for very heavy ions plotted as a function of ion energy is a minimum when the inactivation cross section is a maximum. Also, we show that the effects of inactivation on mutations from light ions is small. In the rest of this paper, we first describe the calculation of inactivation and mutation cross sections in the track model. The model is then fit to the several data sets for inactivation and mutation, and the inactivation and mutation probability as a function of ion charge and energy is discussed.

Inactivation and Mutation Cross Sections in Track Model

In order to introduce the effects of survival probability on the evaluation of mutation cross sections in the track model, we first review the evaluation of the inactivation cross section. The dose response of the system to low LET irradiations for the end point of inactivation (loss of colony forming ability) is assumed to be known and represented by the probability function $P_I(D)$ where D is the absorbed dose in greys. Track structure is understood by finding the spatial distribution of local dose about the path of an ion, as deposited in the sensitive volume elements of the cell. For calculations, the average radial dose as a function of the radial distance t in a short cylinder of radius a_{0I} is used as denoted by $\bar{D}_I(t)$. The inactivation cross section for a single punative target is found by integrating the probability for inactivation evaluated with the average radial dose in a_{0I} over all radial distances, as (Katz et al. 1971)

$$\sigma_I = \int_0^{T_{\max}} 2\pi t \, P_I[\bar{D}_I(t)] \, dt \qquad (1)$$

where t is in units of centimeters and $T_{\max}$ is the maximum range of the delta rays, often denoted the penumbra radius, which is a function of ion velocity β.

In implementing equation (1) for describing survival curves, a multitarget model for low LET dose response is often assumed where

$$P_I(D) = [1 - \exp(-D/D_{0I})]^m \quad (2)$$

where m is the target number and D_{0I} is the low LET characteristic dose at which an average of one hit per target occurs. The surviving fraction of cells after low LET irradiation at D is $N/N_0 = 1 - P_I(D)$. The use of a multitarget model to fit the high dose rate, low LET dose response is convenient in the calculations, and it can be shown that other parametric models will work equally as well in predicting action cross sections for ions using equation (1).

The inactivation cross section evaluated from equation (1) and plotted as a function of the velocity of an ion is observed to reach a plateau at a value of about $1 - 1.4\pi a_{0I}^2$ to mark the transition from the grain-count regime to the track-width regime (Katz et al. 1971). The sensitive targets for $m > 1$ are contained in some volume represented by the cross-sectional area σ_{0I} which may be less than the total cross-sectional area of the cell nucleus. The cross sections calculated by equation (1) are then multiplied by the ratio $\sigma_{0I}/1.4\pi a_{0I}^2$ when $m > 1$. The values of a_{0I} and σ_{0I} are determined by fitting the model equations to an experimental data set with track segment irradiations. In the track model, the surviving fraction after irradiation with track segment ion bombardments is separated into intratrack and intertrack effects as

$$\frac{N}{N_0} = \pi_i \times \pi_\gamma \quad (3)$$

where the intratrack or ion-kill contribution is given by

$$\pi_i = \exp(-\sigma_I F) \quad (4)$$

where F is the fluence of the ion and the intertrack or gamma-kill probability is

$$\pi_\gamma = 1 - P_I(D_\gamma) \quad (5)$$

where D_γ is the gamma-kill dose given by

$$D_\gamma = \left(1 - \frac{\sigma_I}{\sigma_{0I}}\right) F \quad (6)$$

with $D_\gamma = 0$ for $\sigma_I > \sigma_{0I}$.

At sufficiently large fluence, the survival curves resulting from equations (1) to (6) display an exponential tail, and the extrapolated cross section can be found as (Katz et al. 1971)

$$\sigma_{ext} = \sigma_I + \left(1 - \frac{\sigma_I}{\sigma_{0I}}\right) \frac{LET}{D_{0I}} \quad (7)$$

The extrapolated cross section is also termed the "final slope cross section" and is the same as σ_I (the initial slope cross section) only when $\sigma_I > \sigma_{0I}$.

In order to evaluate the mutation cross section in the track model the probability of survival of the cell must be considered in order for the mutation phenotype to be expressed. Unlike the target for inactivation, the target for gene mutation is well localized. For the HPRT mutation assay, this target is on the X chromosome. We assume that the targets for inactivation are located randomly in the cell nucleus (i.e., not chromosome specific). In figure 1, we depict the sites for mutation and inactivation relative to the ion path.

The cross section for mutation is evaluated by considering the dose-response probability per surviving cell for low LET induction of the mutation, denoted P_M, multiplied by the dose-response probability that the cell survives. The product of the mutation frequency per

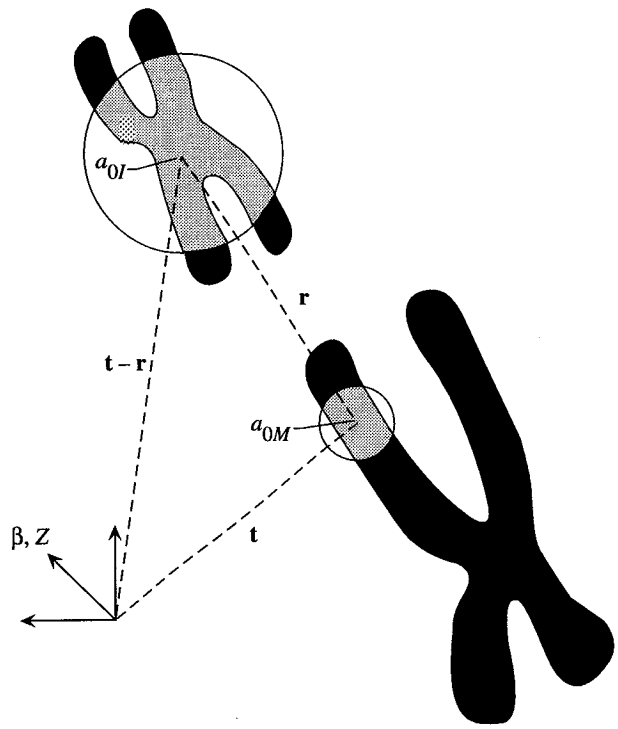

Figure 1. Schematic diagram of correlation of lesion sites for mutation and inactivation relative to path of ion of velocity β and charge Z at impact parameter **t** from mutated gene with **r** displacement of two sites.

survivor P_M times the survival probability $1 - P_I$ represents the number of mutants observed. Track structure is introduced by correlating the location of these events within the cell nucleus. The cross section for production of observable mutants is then

$$\sigma_M = \int_0^{T_{\max}} 2\pi t \, dt \, P_M[\bar{D}_M(t)] \frac{1}{V_N} \int dr \, \{1 - P_I[\bar{D}_I(\mathbf{t} - \mathbf{r})]\} \tag{8}$$

where V_N is the volume of the cell nucleus and the radial dose at the gene, $\bar{D}_M$ is averaged over the mutation site of radius a_{0M}. The success of equation (8), as shown in the calculations later, is to correlate the spatial distributions of lesions for these end points. In calculations, the value of V_N is restricted to account for the finite size of a_{0I} such that the displacement keeps the inactivation sites inside the nuclear volume. We expect the displacement distance then to be localized within about 3 μm from the mutation site. Many factors, such as the finite chromosome number, chromosome geometry, temporal position, preclude any ab initio correlation of the mutation and inactivation lesion sites. Its actual value for calculations is described later.

Radial Dose Model

For calculations of cross sections, the radial dose from secondary electrons based on the model of Kobetich and Katz (1968) is used. Some physical inputs in this calculation have been updated (Cucinotta et al. 1996), including the use of the secondary electron spectrum from proton impact in water from Rudd (1989), a revised angular distribution function, and the electron range-energy and stopping-power formula from Tabata, Ito, and Okabe (1972). Also, a contribution has been included for excitations to the radial dose model by using the function of Brandt and Ritchie (1974), normalized such that the summed contributions from excitations and delta rays (from modified Kobetich and Katz model) conserves the LET for each ion where

$$\text{LET} = 2\pi \int_0^{T_{\max}} t \, dt \, [D_\delta(t) + D_{\text{exc}}(t)] \tag{9}$$

The effects of nuclear stopping power, which should become important at low energies (<1 MeV/u), have not been considered.

The radial dose model used in calculations is based on the model of Kobetich and Katz (1968) and uses recent models for secondary electronic production and the electron range-energy formula and stopping power (Tabata, Ito, and Okabe 1972; Rudd 1989). In this model the radial dose $D(t)$ as a function of the radial distance t from the center of the path of the ion and including an angular distribution for the ejected electrons with energy W at an angle θ is given by

$$D_\delta(t) = \frac{-1}{2\pi t} \sum_i \int d\Omega \int_{\omega_t(\theta)}^{\omega_m - I_i} d\omega \, \frac{\partial}{\partial t} \times [\eta(t,\omega,\theta) \, W(t,\omega,\theta)] \, \frac{dn_i}{d\omega \, d\Omega} \tag{10}$$

where ω_m is the maximum secondary electron energy, I_i is the ionization energy for an electron, η is the transmission function, and W is the residual energy of the electrons. In equation (10), the summation is over all atoms. The range-energy formulas assumed are from Tabata, Ito, and Okabe (1972) and the transmission functions from Kobetich and Katz (1959).

A qualitative model for the angular distribution of the secondary electrons is to assume that a distribution peaked about the classical ejection value, such as

$$\frac{dn}{d\omega \, d\Omega} = \frac{dn}{d\omega} f(\theta) \tag{11}$$

with

$$f(\theta) = \frac{N}{[\theta - \theta_c(\omega)]^2 + (A/\omega)} \tag{12}$$

with $\theta_c(\omega)$ determined as the root of

$$\cos^2\theta = \frac{\omega}{\omega_m} \tag{13}$$

with N a normalization constant and A a constant found to be about 0.015 keV to simulate the data of Rudd, Toburen, and Stolterfoht (1976) and Toburen (1974). The distribution of equations (11) to (13) does not reproduce any forward or backward peaking in the electron production spectrum. For the single differential distribution in equation (11), the model of Rudd (1989) was used for scaling to heavy ions by using effective charge. Extensive comparisons of the model described previously with experiments for radial dose from heavy ions are described in Cucinotta et al. (1995). The use of the model of Rudd and the angular distribution of equations (11) to (13) generally reduces the dose in the core region.

The model for the radial dose from delta rays described previously can be parameterized by utilizing the $1/t^2$ fall-off dependence at intermediate distances and introducing functions that modify the distribution at small and large distances. The radial dose in water is then

$$D_\delta(t) = (Z^{*2}/\beta^2)(Ne^4/m_e c^2) f_s(t)(1/t^2) f_L(t) \tag{14}$$

where βc is the ion velocity, Z^* is the effective charge, N is number, e is electron, and m_e is the electron mass. The function $f_s(t)$ modifies the short distance behavior and is represented by

$$f_s(t) = \left(\frac{10^{-7}}{t} + c_1\right)^{-1} \tag{15}$$

with

$$c_1 = 0.6 + 1.7\beta - 1.1\beta^2 \tag{16}$$

The function $f_L(t)$ modifies the long distance behavior and is represented by

$$f_L(t) = \exp[-(t/0.37T_{\max})^2] \tag{17}$$

where $T_{\max}$ is the maximum radial penetration distance for delta rays of an ion at speed βc.

The radial dose from excitations is assumed to be in the form (Brandt and Ritchie 1974)

$$D_{\exp}(t) = \frac{C \exp(-t/d)}{t^2} \tag{18}$$

where C is determined by normalizing to the total LET from equation (9) and $d = \beta/2\omega_r$ with $\omega_r = 13$ eV for water. The radial dose contribution from excitations is then contained to small radii of less than a few 10 nm.

The results of our calculations, for 1-MeV protons and ^{20}Ne at 377 MeV/amu in water, using different assumptions are shown in figure 2. Also shown in figures 2(a) and 2(b) are measurements by Wingate and Baum (1976) for protons and measurements by Varma and Baum (1980) for Ne, respectively. The present calculations made for other ions (adjusted from calculations for protons by multiplication with the square of the effective charge) are used for the evaluation of action cross sections. Typically different assumptions yield

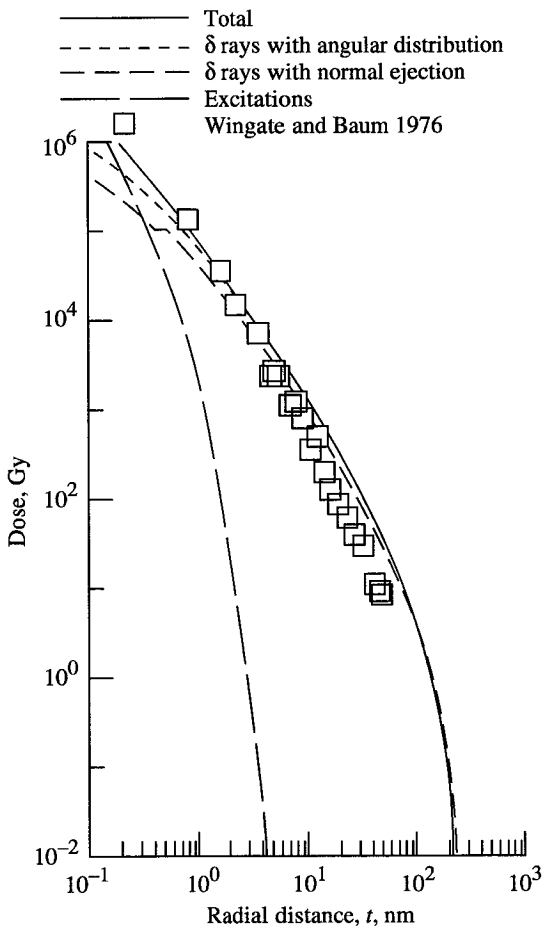

(a) Protons at 1 MeV in water.

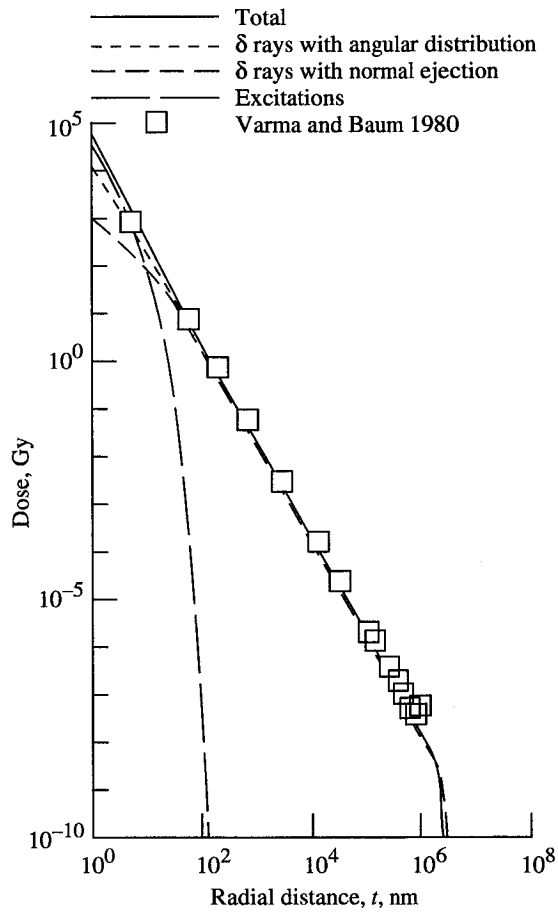

(b) ^{20}Ne at 397 MeV/amu.

Figure 2. Radial dose distribution calculated with different assumptions.

major differences close to the ion path (most important for latent tracks and possibly for consideration of damage to crystalline structure) and remote from the ion path (most important for considerations of "thin down," the decrease in the inactivation cross section while the ion LET increases, as the ion approaches the end of its range). A comparison using equations (14) to (17) for the radial dose from secondary electrons and the model of equations (10) to (13) is shown in figure 3 where $t^2D(t)$ is plotted; good agreement is found.

Comparisons for Inactivation Cross Sections

We first discuss calculations and comparisons with experiment for the inactivation of *E. Coli B/r*, *E. Coli* $B_{s\text{-}1}$, and *Bacillus Subtilis* spores (Katz, Cucinotta, and Zhang 1996). Values of D_0 for γ rays for these cells differ among different investigators. Thus for *B/r*, Takahashi et al. (1986) find 36.5 Gy, whereas Schäfer, Schmitz, and Bücker (1994) find 47.6 Gy. We have chosen a value of 40 Gy for best fit of our calculations to the heavy ion data (Schäfer, Schmitz, and Bücker 1994). For $B_{s\text{-}1}$, Takahashi reports 12.6 Gy, whereas Schäfer reports 15.4 Gy. For this report, we have chosen 12.6 Gy for best fit of calculations to data. Calculated cross sections for a variety of heavy ion bombardments are shown in figures 4(a) and 4(b), with data points superimposed.

For the inactivation of *Bacillus subtilis* spores of strain rec$^-$, we have chosen $D_0 = 110$ Gy as compared with the experimental value of 93 ± 7.6 Gy. Calculated cross sections versus LET are shown in figure 4(c) with data from Baltschukat and Horneck (1991) superimposed. In figure 4(d) calculations for the inactivation of *Bacillus subtilis* spores (wild) have been shown with data from Baltschukat and Horneck (1991) and Donnellan and Morowitz (1957) superimposed. We have used $m = 2$ and $D_0 = 222$ Gy and have included in figure 4(d) the misrepair term to the cross section as described in Wilson, Cucinotta, and Shinn (1993). In figure 5, we show calculations and data for inactivation cross sections of wild-type spores of *Bacillus subtilus* versus the ion energy where the gamma-ray response is parameterized by using a linear kinetics model of repair/misrepair. The application of the linear kinetics model in evaluating action cross sections is seen to be most important at low ion energy where a second maximum in the inactivation cross section is predicted because of misrepair in agreement with the data of Schneider, Kost, and Schäfer (1990). The higher energy maximum in the cross section is at the velocity where delta rays are most efficient but also dependent on the density of the track. Below a few MeV/amu, the range of the delta rays becomes smaller than the size of important targets in the cell nucleus, and thin down occurs.

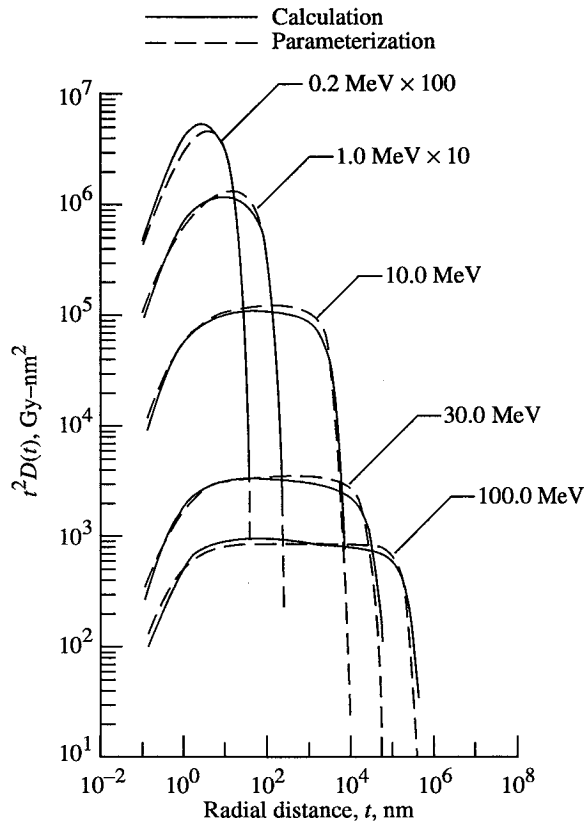

Figure 3. Calculations of radial dose from parameterization of equations (14) to (17) and calculations on which it is based.

Inactivation as a function of impact parameter has been measured for 1.4 MeV/amu heavy ion beams (Weisbrod et al. 1992) using wild-type strain spores. In figure 6 we compare these measurements with the present model. In one set of calculations (the upper set of curves), we consider the experiment impact parameter relative to the sensitive site in the spore. Here there is unit probability for inactivation following uranium bombardment to about 0.2 μm and for nickel bombardment to about 0.15 μm. Note that this is different from the results found by Weisbrod et al. (1992) with the earliest version of the Katz model (Butts and Katz 1967), where a one-hit response and a simplified radial dose model are assumed. With this earlier version of the Katz model, the inactivation probability for uranium was found to be unity for larger impact parameters than found here, and the electron range is underestimated. In the lower set of curves, we have used the estimates of the size of the spore to average the inactivation probability according to a random location for the sensitive volume in the spores. We have averaged over two short cylinders of radius corresponding to the estimated minor (0.18 μm) and major (0.36 μm) radii of an ellipsoid-shaped spore (Weisbrod et al. 1992). The lower set of curves is in much better agreement with the experiment, and it is expected that

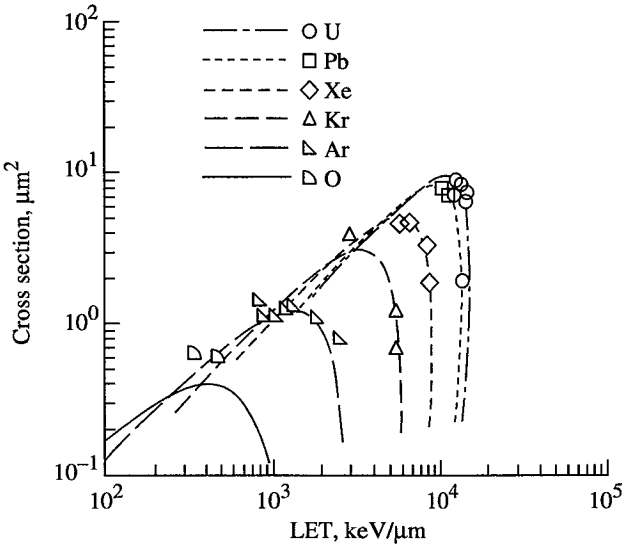

(a) *E. Coli B/r*; $m = 1$; $D_{0I} = 40$ Gy; $a_{0I} = 0.1$ μm; superimposed data from Schäfer, Schmitz, and Bücker 1994.

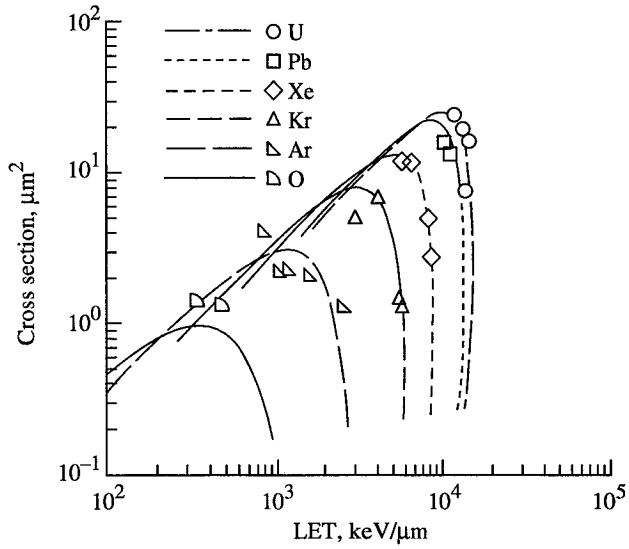

(b) *E. Coli* B_{s-1}; $m = 1$; $D_{0I} = 12.6$ Gy; $a_{0I} = 0.1$ μm; superimposed data from Schäfer, Schmitz, and Bücker 1994.

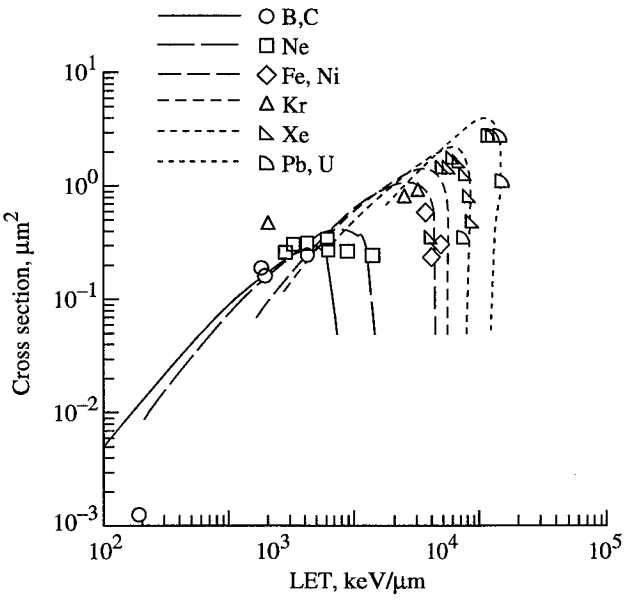

(c) *Bacillus subtilis* (rec) spores; $m = 1$; $D_{0I} = 110$ Gy; $a_{0I} = 0.3$ μm; superimposed data from Baltschukat and Horneck 1991.

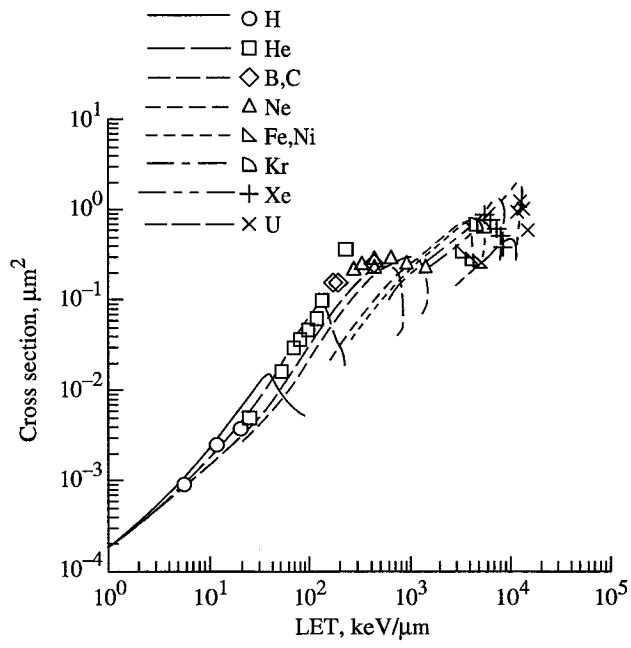

(d) *Bacillus subtilis* (wild) spores; $m = 2$; $D_{0I} = 222$ Gy; $a_{0I} = 0.3$ μm; superimposed data from Baltschukat and Horneck 1991; Donnellan and Morowitz 1957.

Figure 4. Calculated inactivation cross sections. m is target number, D_{0I} is characteristic dose, and a_{0I} is target radius.

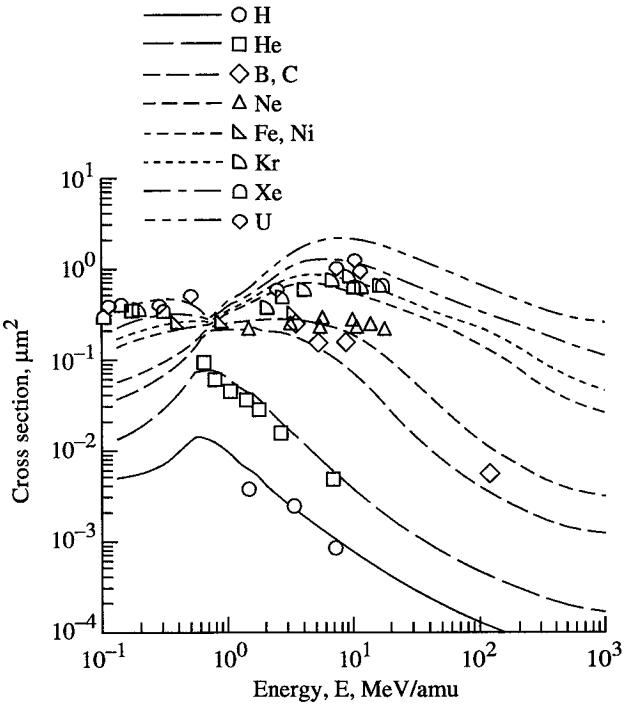

Figure 5. Calculated inactivation cross section for *Bacillus subtilis* (wild) spores versus ion energy using repair kinetics model.

details of the geometry of the spores and the sensitive sites are required for further improvements of calculations to experiment.

Comparisons for Mutation Cross Sections

We next consider the cross sections for HPRT mutations in V79 cells. For survival, the X-ray response parameters as well as the geometric parameters have been fitted by Katz et al. (1994) as listed in table 1. For HPRT mutations the X-ray response in V79 cells has been measured by Kranert, Schneider, and Kiefer (1990) for doses of 1 to 10 Gy. The multitarget model can be applied directly to the mutation frequency as shown by the solid line in figure 7 with the resulting parameters $m = 2$, $D_{0M} = 950$ Gy. Wilson, Cucinotta, and Shinn (1993) formulated a linear kinetics model of repair/misrepair to treat multiple lesion types such as mutation and inactivation and which also considers dose-rate effects. The fit of this model to the X-ray data is shown by the dashed line in figure 7. For our purpose of treating track structure effects on evaluating mutation cross sections, the use of the multitarget model or linear kinetics model for mutations gave similar fits to the data. The multitarget model is used in the figures discussed later.

Calculations of inactivation cross sections for V79 cells and experimental data are presented versus LET in figure 8. Shown are the final slope or extrapolated cross

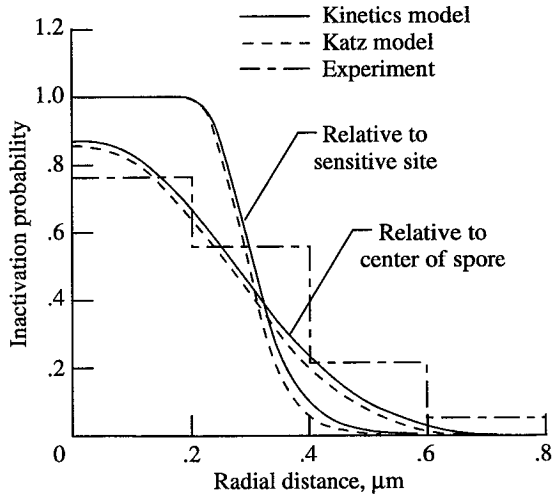

(a) Uranium at 1.4-MeV/amu energy.

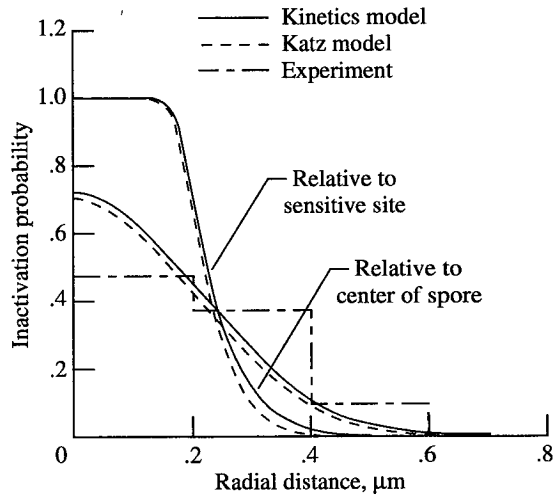

(b) Nickel at 1.4-MeV/amu energy.

Figure 6. Calculation versus experimental histograms (Facius et al. 1983) for *Bacillus subtilis* spore inactivation versus impact parameter.

Table 1. Cellular Response Parameters for V79 Cells

End point	m	D_0, Gy	σ_0, μm²	a_0, nm
Inactivation	3	1.82	42.8	820
HPRT mutations	2	950	6.5×10^{-3}	50

sections for several charges. Cellular response parameters for inactivation (Katz et al. 1994) are presented in table 1. The maximum value of the inactivation cross section versus LET for each specific ion occurs in the energy range of about 5 to 30 MeV/amu. The decrease in the inactivation cross sections is called "thin down" and occurs when the value of $T_{max} < a_{01}$. The nuclear area

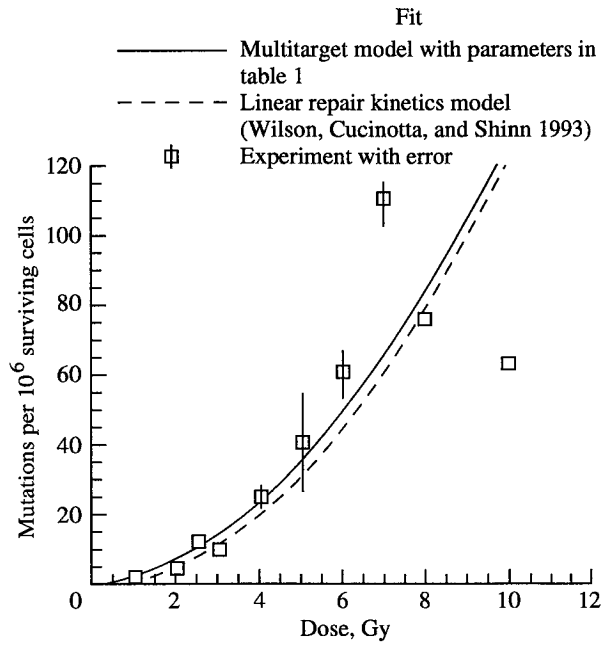

Figure 7. Dose response for number of mutations per 10^6 surviving cells for HPRT mutations in V79 cells. Data from Kranert, Schneider, and Kiefer 1990; $m = 2$; $D_{0M} = 950$ Gy.

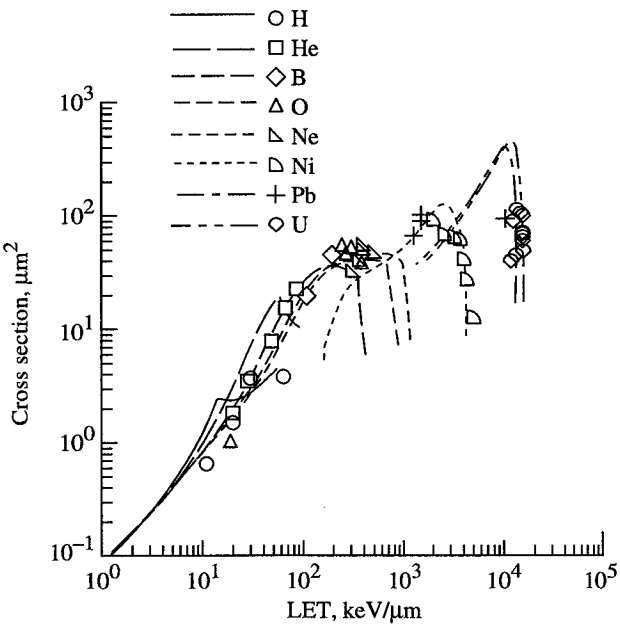

Figure 8. Calculations and experimental values of inactivation cross sections (final slope) for V79 cells versus LET. Data from Thacker, Stretch, and Stephens 1979; Kranert, Schneider, and Kiefer 1990; Belli et al. 1993; Kiefer, Stoll, and Schneider 1994.

for V79 cells has been reported as 130 μm^2 (Goodhead et al 1980), which is roughly three times the value of σ_{0I} = 42.8 μm^2. We note that for a small range of energies and for very large charges, the model inactivation cross sections exceed 130 μm^2.

In the evaluation of mutation cross sections by equation (8) the upper limit on r should be on the order of 1 to 3 μm in view of the measured nuclear area for V79 cells and the fitted values of σ_{0I} and a_{0I}. We have treated the maximum value of r, denoted r_{max}, as a fitting parameter estimated as r_{max} = 1.75 μm from calculations. We first show plots of σ_M for uranium and oxygen ions versus energy in figure 9 for several fixed values of r. For small values of r, virtually no mutations are seen for heavy ions of modest energies where the highest rates of inactivation occur. At low energies (below 1 MeV/amu), the mutation cross sections increase where thin down in the inactivation cross sections occurs. A second maximum in the inactivation cross section in yeast and bacteria has been observed at low energies (Schneider, Kost, and Schäfer 1990) which is not accounted for by the delta-ray model and would most likely reduce the mutation cross sections in the energy region from 0.1 to 1.0 MeV/amu from the calculations shown if the same effect is present for the inactivation of V79 cells.

In figure 10 we show the model calculations and experimental values for V79 mutation cross sections versus ion energy for several ion types. The data shown for heavy ions with $Z > 8$ are from Kranert, Schneider, and Kiefer (1990) and Kiefer, Stoll, and Schneider (1994). The data shown for He and B are the initial slope cross sections from Thacker, Stretch, and Stephens (1979); the data for protons, from Belli et al. (1993). Different strains of V79 cells are used by the authors noted. Cellular response parameters for mutation are given in table 1. The value of a_{0M} most strongly affects the fit for light-charged ions and is somewhat sensitive to the angular distribution of secondary electrons assumed in calculations. The value of a_{0M} obtained by fits, as noted by Goodhead (1989), corresponds to a large portion of the HPRT gene. The agreement between calculations and experiment is good. Heavy ions are seen to display minima in their mutation capability due to inactivation effects. These minima occur for kinetic energies from a few MeV/amu to about 30 MeV/amu. The overestimation of the model inactivation cross section for uranium in this energy regime affects the mutation cross sections too severely; however, the trends are correct. Relativistic heavy ions thus become more effective for mutation induction because of the large radial extent of their tracks from delta rays. The spreading of the ion track at high energies reduces the effects of inactivation; thus, the likelihood of mutation is increased. Note also that ions of moderate charge become more efficient than higher charge ions in the moderate energy region from about 5 to 50 MeV/amu. Light ions are only mildly affected by inactivation effects.

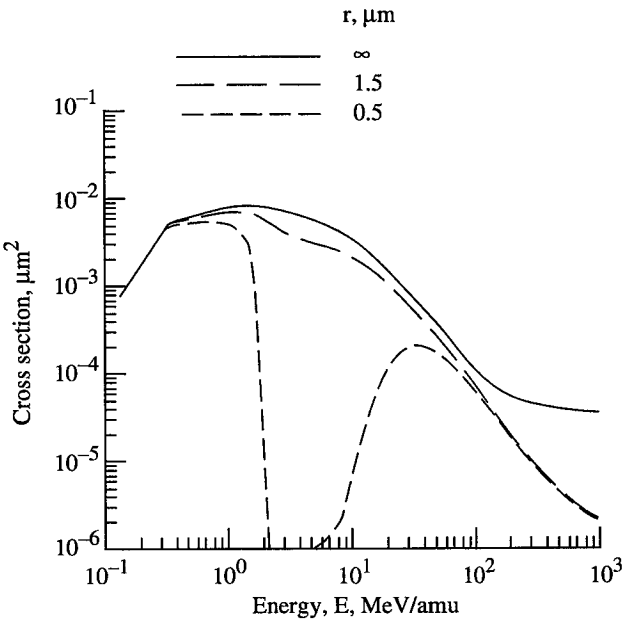

(a) Oxygen.

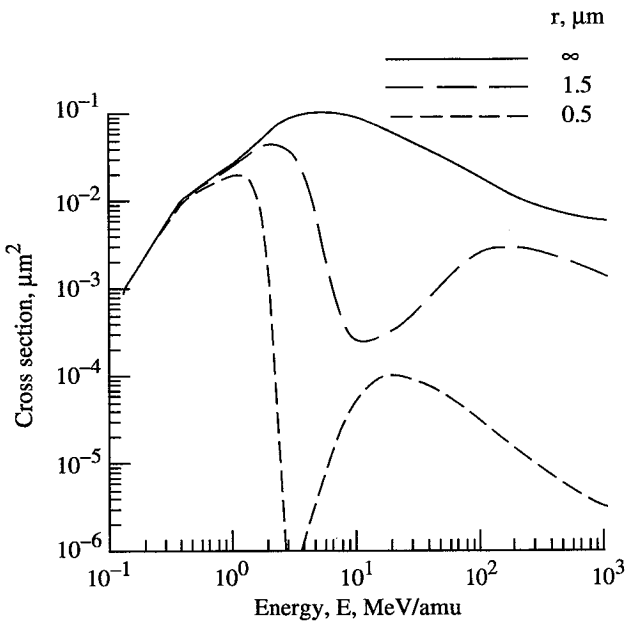

(b) Uranium.

Figure 9. Calculations of mutation cross sections versus energy at various fixed separation distances from mutation lesion site to inactivation lesion site.

In figure 11 we show the mutation cross sections versus LET. A "hook" structure distinct from the hooks seen in inactivation cross sections because of thin-down effects is observed. A minimum in the mutation cross section for heavy ions is seen at the LET value corresponding to the maximum inactivation probability. A sharp rise in σ_M is seen for a narrow band of LET as

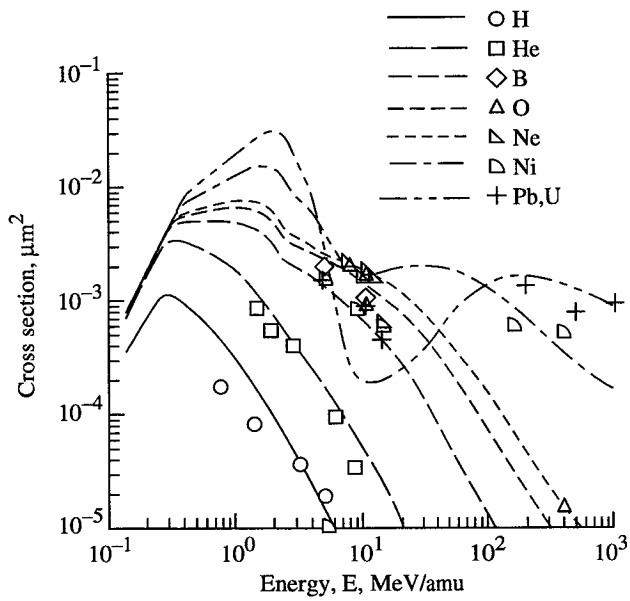

Figure 10. Calculations and experimental values of mutation cross sections versus energy for HPRT mutations in V79 cells. Data from Thacker, Stretch, and Stephens 1979; Kranert, Schneider, and Kiefer 1990; Belli et al. 1993; Kiefer, Stoll, and Schneider 1994.

correlated with the thin down of σ_I for the same LET band. The complicated structure of σ_M predicted by the model prohibits the use of a single quantity such as LET or Z^{*2}/β^2 for defining radiation quality.

Cross sections for HPRT mutations have also been reported for human fibroblast cells (Cox and Masson 1979; Tsuboi, Yang, and Chen 1992) and for human B-lymphoblastoid cells (Kronenberg and Little 1989; Kronenberg 1994). The response of fibroblasts and lymphoblasts to heavy ions has been noted to be quite different by Kronenberg (1994) as seen, for example, in the large differences in cross sections for relativistic iron nuclei of similar energies where the cross sections in fibroblasts are about a factor of 15 larger in the human fibroblasts. The present models suggest that these differences are inherent in the gamma-ray response without regard to any specific expression pathways for heavy ions. In table 2, we list reported initial slope estimates and cross-sectional geometric areas for several cell types in which HPRT mutations have been measured. We note that the low LET response is different, larger for the human fibroblasts and similar for the V79 and lymphoblasts. Also, the measured cross-sectional area of the human fibroblast is about twice as large as that of the V79 and lymphoblasts. If the multitarget model is fit to the human fibroblast data with $m = 2$, a value of about $D_{0M} = 650$ Gy is found which compares with the 950 Gy found for V79 cells. Also, calculations for an

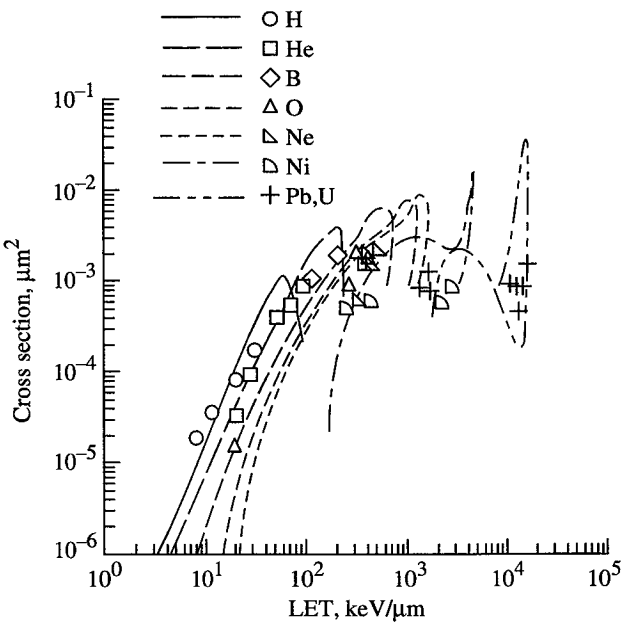

Figure 11. Calculations and experimental values of mutation cross sections versus LET for HPRT mutations in V79 cells. Data from Thacker, Stretch, and Stephens 1979; Kranert, Schneider, and Kiefer 1990; Belli et al. 1993; Kiefer, Stoll, and Schneider 1994.

Table 2. Photon Initial Slopes and Geometric Parameters for Several Cell Lines

Cell type	Initial slope for HPRT mutations, cGy^{-1}	Geometric area, μm^2	Radius, μm
V79	0.35×10^{-7}	130	6.4
Human lymphoblasts	0.6	87	5.3
Human fibroblasts	2.3	220	8.4

earlier model (Cucinotta and Wilson 1994) which neglected inactivation effects were in disagreement with the data of Tsuboi, Yang, and Chen (1992) for Fe and La nuclei. In the cross-section formula of equation (8), the values of V_N are also expected to be increased for the larger nucleus of the human fibroblast cells; thus, the role of inactivation on the evaluation of mutation cross sections was slightly reduced. We expect that the differences in low LET response to be sufficient to explain the differences in mutation rates between cell lines without the introduction of any new mechanisms for ions. The recent measurements of Kiefer, Stoll, and Schneider (1994) using nickel with energy of 400 MeV/amu support this premise where the mutation cross section in V79 cells is 5.0×10^{-4} μm^2 in comparison with iron nuclei with energy of 600 MeV/amu in lymphoblasts and fibroblasts with mutation cross sections of 3.7×10^{-4} μm^2 and 56.5×10^{-4} μm^2, respectively.

Concluding Remarks

The track structure model uses a model fit to experimental measurements for high dose-rate response to low LET (linear energy transfer) radiations, the radial dose distribution about the path of a heavy ion, and a few geometric parameters to predict the effects of the identical system to an arbitrary ion. In the past this procedure has been shown to be quite successful for describing inactivation cross sections in many biological samples. The earlier calculations have been improved by using improved models of the radial dose distribution and good agreement was found with recent experiments. Herein we have shown that a similar procedure can be applied to predict mutation rates when the effects of inactivation are included by spatially correlating lesion sites. The continued success of the track model in fitting biological data with ion beams suggests that a fundamental approach to biological damage from energetic photons would provide much of the understanding needed for ion beams as well. The action cross sections for mutation versus LET will have a distinct structure due to the effects of inactivation, especially for heavy ions. The use of a single parameter such as LET or Z^{*2}/β^2 (where Z^* is the effective charge number and β is the ion velocity) to represent radiation quality is thus even less accurate for mutations than inactivation. This result suggests important implications for space radiation shielding studies.

NASA Langley Research Center
Hampton, VA 23681-2199
January 10, 1997

References

Baltschukat, K.; and Horneck, G. 1991: Responses to Accelerated Heavy Ions of Spores of *Bacillus-Subtilis* of Different Repair Capacity. *Radiat. & Environ. Biophys.*, vol. 30, no. 2, pp. 87–104.

Belli, M.; Cera, F.; Cherubini, R.; Haque, A. M. I.; Ianzini, F.; Moschini, G.; Sapora, O.; Simone, G.; Tabocchini, M. A.; and Tiveron, P. 1993: Inactivation and Mutation Induction in V79 Cells by Low Energy Protons: Re-Evaluation of the Results at the LNL Facility. *Int. J. Radiat. Biol.*, vol. 63, no. 3, pp. 331–337.

Brandt, Werner; and Ritchie, R. H. 1974: Primary Processes in the Physical Stage. *Physical Mechanisms in Radiation Biology*, R. D. Cooper and R. Wood, eds., Tech. Info. Center, U.S. Atomic Energy Commission, pp. 20–49.

Butts, J. J.; and Katz, Robert 1967: Theory of RBE for Heavy Ion Bombardment of Dry Enzymes and Viruses. *Radiat. Res.*, vol. 30, no. 4, pp. 855–871.

Cox, Roger; and Masson, W. K. 1979: Mutation and Inactivation of Cultured Mammalian Cells Exposed to Beams of Accelerated Heavy Ions. *Int. J. Radiat. Biol.*, vol. 36, no. 2, pp. 149–160.

Cucinotta, Francis A.; and Wilson, John W. 1994: *Estimates of Cellular Mutagenesis From Cosmic Rays*. NASA TP-3453.

Cucinotta, Francis A.; Katz, Robert; Wilson, John W.; and Dubey, Rajendra R. 1995: *Heavy Ion Track-Structure Calculations for Radial Dose in Arbitrary Materials*. NASA TP-3497.

Cucinotta, F. A.; Wilson, J. W.; Katz, R.; Atwell, W.; Badhwar, G. D.; and Shavers, M. R. 1996: Track Structure and Radiation Transport Model for Space Radiobiology Studies. *Adv. Space Res.*, vol. 18, no. 12, pp. (12)183–(12)194.

Donnellan, J. Edward, Jr.; and Morowitz, Harold J. 1957: The Irradiation of Dry Spores of *Bacillus Subtilis* With Fast Charged Particles. *Radiat. Res.*, vol. 7, pp. 71–78.

Facius, R.; Schaefer, M.; Baltschukat, K.; and Buecker, H. 1983: Inactivation Probability of Heavy Ion-Irradiated *Bacillus Subtilis* Spores as a Function of the Radial Distance to the Particle's Trajectory. *Adv. Space Res.*, vol. 3, no. 8, pp. 85–94.

Goodhead, D. T.; Munson, R. J.; Thacker, J.; and Cox, R. 1980: Mutation and Inactivation of Cultured Mammalian Cells Exposed to Beams of Accelerated Heavy Ions—4. Biophysical Interpretation. *Int. J. Radiat. Biol. & Relat. Studies Phys. Chem. & Med.*, vol. 37, no. 2, pp. 135–168.

Goodhead, Dudley T. 1989: Relationships of Radiation Track Structure to Biological Effect: A Re-Interpretation of the Parameters of the Katz Model. *Nucl. Tracks Radiat. Meas.*, vol. 16, no. 2/3, pp. 177–184.

Grahn, Douglas, ed. 1973: HZE-Particle Effects in Manned Spaceflight. Space Science Board, National Research Council, National Academy of Sciences.

Katz, R.; Ackerson, B.; Homayoonfar, M.; and Sharma, S. C. 1971: Inactivation of Cells by Heavy Ion Bombardment. *Radiat. Res.*, vol. 47, pp. 402–425.

Katz, R.; Dunn, D. E.; and Sinclair, G. L. 1985: Thindown in Radiobiology. *Radiat. Prot. Dosim.*, vol. 13, no. 1–4, pp. 281–284.

Katz, R.; Zachariah, R.; Cucinotta, F. A.; and Zhang, C. X. 1994: Survey of Cellular Radiosensitivity Parameters. *Radiat. Res.*, vol. 140, no. 3, pp. 356–365.

Katz, Robert; Cucinotta, Francis A.; and Zhang, C. X. 1996: The Calculation of Radial Dose From Heavy Ions: Predictions of Biological Action Cross Sections. *Nucl. Instrum. & Methods Phys. Res. B*, vol. 107, no. 1–4, pp. 287–291.

Kiefer, Jürgen 1993: Theoretical Analysis of Heavy Ion Action on Cells: Model-Free Approaches, Consequences for Radiation Protections. *Biological Effects and Physics of Solar and Galactic Cosmic Radiation*, Part A, Charles W. Swenberg, Gerda Horneck, and E. G. Stassinopoulos, eds., Plenum Press, pp. 283–290.

Kiefer, J.; Stoll, U.; and Schneider, E. 1994: Mutation Induction by Heavy Ions. *Adv. Space Res.*, vol. 14, no. 10, pp. 257–265.

Kobetich, E. J.; and Katz, R. 1959: Electron Energy Dissipation. *Nucl. Instrum. Methods*, vol. 71, no. 2, pp. 226–230.

Kobetich, E. J.; and Katz, Robert 1968: Energy Deposition by Electron Beams and δ Rays. *Phys. Rev.*, vol. 170, no. 2, pp. 391–396.

Kost, Michael; and Kiefer, Jürgen 1993: Biological Action of Single Heavy Ions on Individual Yeast Cells. *Biological Effects and Physics of Solar and Galactic Cosmic Radiation*, Part A, Charles E. Swenberg, Gerda Horneck, and E. G. Stassinopoulos, eds., Plenum Press, pp. 117–123.

Kranert, T.; Schneider, E.; and Kiefer, J. 1990: Mutation Induction in V79 Chinese Hamster Cells by Very Heavy Ions. *Int. J. Radiat. Biol.*, vol. 58, no. 6, pp. 975–987.

Kronenberg, A.; and Little, J. B. 1989: Locus Specificity for Mutation Induction in Human Cells Exposed to Accelerated Heavy Ions. *Int. J. Radiat. Biol.*, vol. 55, no. 6, pp. 913–924.

Kronenberg, A. 1994: Mutation Induction in Human Lymphoid Cells by Energetic Heavy Ions. *Adv. Space Res.*, vol. 14, no. 10, pp. 339–346.

Lett, J. T.; Cox, A. B.; and Story, M. D. 1989: The Role of Repair in the Survival of Mammalian Cells From Heavy Ion Irradiation—Approximation to the Ideal Case of Target Theory. *Adv. Space Res.*, vol. 9, no. 10, pp. 99–104.

Little, John B. 1994: Changing Views of Cellular Radiosensitivity. *Radiat. Res.*, vol. 140, no. 3, pp. 299–311.

Loeb, Lawrence A. 1991: Mutator Phenotype May Be Required for Multistage Carcinogenesis. *Cancer Res.*, vol. 51, pp. 3075–3079.

National Council on Radiation Protection Measurements 1990: *The Relative Biological Effectiveness of Radiations of Different Quality*. NCRP No. 104.

Rudd, M. E.; Toburen, L. H.; and Stolterfoht, N. 1976: Differential Cross Sections for Ejection of Electrons From Helium by Protons. *Atomic Data and Nucl. Data Tables*, vol. 18, no. 5, pp. 413–432.

Rudd, M. Eugene 1989: User-Friendly Model for the Energy Distribution of Electrons From Proton or Electron Collisions. *Nucl. Tracks Radiat. Meas.*, vol. 16, no. 2/3, pp. 213–218.

Schäfer, M.; Schmitz, C.; and Bücker, H. 1994: DNA Double Strand Breaks Induced in *Escherichia Coli* Cells by Radiations of Different Quality. *Radiat. Prot. Dosim.*, vol. 52, no. 1–4, pp. 233–236.

Schneider, E.; Kost, M.; and Schäfer, M. 1990: Inactivation Cross Sections of Yeast and Bacteria Exposed to Heavy Ions of Low Energy (<600 keV/u). *Radiat. Prot. Dosim.*, vol. 31, no. 1/4, pp. 291–295.

Tabata, T.; Ito, R.; and Okabe, S. 1972: Generalized Semiempirical Equations for the Extrapolated Range of Electrons. *Clear Instum. & Methods*, vol. 103, pp. 85–91.

Takahashi, T.; Yatagai, F.; Konno, S.; Katayama, T.; and Kaneko, I. 1986: Microdosimetric Considerations of Effects of Heavy Ions on Microorganisms. *Adv. Space Res.*, vol. 6, no. 11, pp. 117–125.

Thacker, John; Stretch, Albert; and Stephens, Miriam A. 1979: Mutation and Inactivation of Cultured Mammalian Cells Exposed to Beams of Accelerated Heavy Ions. II. Chinese Hamster V79 Cells. *Int. J. Biol.*, vol. 36, no. 2, pp. 137–148.

Toburen, L. H. 1974: Distribution in Energy and Angle of Electrons Ejected From Xenon by 0.3- to 2.0-MeV Protons. *Phys. Rev. A*, vol. 9, no. 6, pp. 2505–2517.

Todd, Paul 1983: Unique Biological Aspects of Radiation Hazards—An Overview. *Adv. Space Res.*, vol. 3, no. 8, pp. 187–194.

Tsuboi, Koji; Yang, Tracy C.; and Chen, David J. 1992: Charged-Particle Mutagenesis—I. Cytoxic and Mutagenic Effects of High-LET Charged Iron Particles on Human Skin Fibroblasts. *Radiat. Res.*, vol. 129, pp. 171–176.

Ullrich, R. L. 1984: Tumor Induction in BALB/c Mice After Fractionated or Protracted Exposures to Fission-Spectrum Neutrons. *Radiat. Res.*, vol. 97, pp. 587–597.

Varma, Matesh N.; and Baum, John W. 1980: Energy Deposition in Nanometer Regions by 377 MeV/Nucleon ^{20}Ne Ions. *Radiat. Res.*, vol. 81, pp. 355–363.

Vogelstein, Bert; and Kinzler, Kenneth W. 1993: The Multistep Nature of Cancer. *Trends Genet.*, vol. 9, no. 4, pp. 138–141.

Weinberg, R. A. 1991: Tumor Suppressor Genes. *Science*, vol. 252, no. 5035, pp. 1138–1145.

Weisbrod, U.; Bücker, H.; Horneck, G.; and Kraft, G. 1992: Heavy-Ion Effects on Bacteria Spores: The Impact Parameter Dependence of the Inactivation. *Radiat. Res.*, vol. 129, pp. 250–257.

Wilson, John W.; Cucinotta, F. A.; and Shinn, J. L. 1993: Cell Kinetics and Track Structure. *Biological Effects and Physics of Solar and Galactic Cosmic Radiation*, Part A, Charles E. Swenbert, Gerda Horneck and E. G. Stassinopoulos, eds., Plenum Press, pp. 295–338.

Wingate, Catharine L.; and Baum, John W. 1976: Measured Radial Distributions of Dose and LET for Alpha and Proton Beams in Hydrogen and Tissue-Equivalent Gas. *Radiat. Res.*, vol. 65, pp. 1–19.

REPORT DOCUMENTATION PAGE

Form Approved
OMB No. 0704-0188

Public reporting burden for this collection of information is estimated to average 1 hour per response, including the time for reviewing instructions, searching existing data sources, gathering and maintaining the data needed, and completing and reviewing the collection of information. Send comments regarding this burden estimate or any other aspect of this collection of information, including suggestions for reducing this burden, to Washington Headquarters Services, Directorate for Information Operations and Reports, 1215 Jefferson Davis Highway, Suite 1204, Arlington, VA 22202-4302, and to the Office of Management and Budget, Paperwork Reduction Project (0704-0188), Washington, DC 20503.

1. AGENCY USE ONLY *(Leave blank)*	2. REPORT DATE	3. REPORT TYPE AND DATES COVERED
	July 1997	Technical Paper

4. TITLE AND SUBTITLE
Calculation of Heavy Ion Inactivation and Mutation Rates in Radial Dose Model of Track Structure

5. FUNDING NUMBERS
WU 199-45-16-11

6. AUTHOR(S)
Francis A. Cucinotta, John W. Wilson, Mark R. Shavers, and Robert Katz

7. PERFORMING ORGANIZATION NAME(S) AND ADDRESS(ES)
NASA Langley Research Center
Hampton, VA 23681-2199

8. PERFORMING ORGANIZATION REPORT NUMBER
L-17579

9. SPONSORING/MONITORING AGENCY NAME(S) AND ADDRESS(ES)
National Aeronautics and Space Administration
Washington, DC 20546-0001

10. SPONSORING/MONITORING AGENCY REPORT NUMBER
NASA TP-3630

11. SUPPLEMENTARY NOTES
Cucinotta and Wilson: Langley Research Center, Hampton, VA; Shavers: Texas A & M University, College Station, TX; Katz: University of Nebraska, Lincoln, NE.

12a. DISTRIBUTION/AVAILABILITY STATEMENT
Unclassified–Unlimited
Subject Category 52
Availability: NASA CASI (301) 621-0390

12b. DISTRIBUTION CODE

13. ABSTRACT *(Maximum 200 words)*
In the track structure model, the inactivation cross section is found by summing an inactivation probability over all impact parameters from the ion to the sensitive sites within the cell nucleus. The inactivation probability is evaluated by using the dose response of the system to gamma rays and the radial dose of the ions and may be equal to unity at small impact parameters. We apply the track structure model to recent data with heavy ion beams irradiating biological samples of *E. Coli, B. Subtilis* spores, and Chinese hamster (V79) cells. Heavy ions have observed cross sections for inactivation that approach and sometimes exceed the geometric size of the cell nucleus. We show how the effects of inactivation may be taken into account in the evaluation of the mutation cross sections in the track structure model through correlation of sites for gene mutation and cell inactivation. The model is fit to available data for HPRT (hypoxanthine guanine phosphoribosyl transferase) mutations in V79 cells, and good agreement is found. Calculations show the high probability for mutation by relativistic ions due to the radial extension of ions track from delta rays. The effects of inactivation on mutation rates make it very unlikely that a single parameter such as LET (linear energy transfer) can be used to specify radiation quality for heavy ion bombardment.

14. SUBJECT TERMS
Biophysics; High-energy ions; Protection

15. NUMBER OF PAGES
14

16. PRICE CODE
A03

17. SECURITY CLASSIFICATION OF REPORT	18. SECURITY CLASSIFICATION OF THIS PAGE	19. SECURITY CLASSIFICATION OF ABSTRACT	20. LIMITATION OF ABSTRACT
Unclassified	Unclassified	Unclassified	